Journal of Thermal Stresses, 27: 433–454, 2004

ISSN: 0149-5739 print/1521-074X online
DOI: 10.1080/01495730490442783

Taylor & Francis
Taylor & Francis Group

CONTACT PHENOMENA IN BRAKING AND ACCELERATION OF BUSH-SHAFT SYSTEM

Jan Awrejcewicz and Yuriy Pyryev
Department of Automatics and Biomechanics (K-16)
Technical University of Łódź
Łódź, Poland

In this work a new one-dimensional model of thermoelastic inertial contact of a braking pad and a rotating inertial shaft, in the braking or accelerating process, is presented and analyzed. Besides dry friction, frictional heat is generated between the two given bodies in contact. The dynamics of the considered system is governed by two non-linear differential equations and one non-linear integral equation. The stability of static solutions, as well as the behavior of contact characteristics in braking and acceleration are analysed.

Keywords friction, frictional heat generation, rigid bush, rotating shaft, stick-slip vibrations, thermoelastic contact.

Friction, frictional heat generation, and heat expansion are all complex phenomena interacting with each other and creating one process in a frictional kinematic pair. Any nonstationary frictional process is characterized by a change over time of all interdependent parameters of the frictional process. In this work it is examined whether the frictional heat generation in a system consisting of a shaft and a friction pad may (and if so, then to what extent) influence the movement of a shaft-attached bush during the braking and acceleration of the shaft. A brief review of the works in the field of frictional heating in thermoelastic contact is given in the literature [1]. In the majority of theoretical works devoted to this problem only periodic self-excited oscillations are considered [2–6]. A method of dry friction investigation, as well as computational approaches leading to its qualitative and quantitative estimation, are reported in the literature [4, 5, 7]. Frictional oscillating processes accompanied by heat transfer have not been investigated so far. It is clear that an investigation into

Received 6 July 2002; accepted 11 June 2003.
The investigations presented in this work were supported by the Polish Committee for Scientific Research (grant no. T07A 019 23). We thank Prof. R. B. Hetnarski for his proper comments and suggestions to improve the paper.
Address correspondence to Prof. Jan Awrejcewicz, Department of Automatics and Biomechanics (K-16), Technical University of Łódź, 1/15 Stefanowskiego St., 90–924 Łódź, Poland. E-mail: awrejcew@ck-sg.p.lodz.pl

NOMENCLATURE

a_1	thermal diffusivity
B_1, B_2	moments of inertia of the shaft and the bush, respectively
Bi	Biot number
E_1	Young's modulus of the shaft
$f(V_w)$	friction coefficient
$f_k(V_w)$	kinetic friction coefficient
f_s	maximum value of the static friction coefficient
$F(\dot{\phi} - \dot{\varphi})$	kinematic friction coefficient depending on relative velocity
$F_t(t)$	dry friction
$h_M(t)$	prescribed dimensionless moment acting on the shaft
$h_T(t)$	environment temperature for Newton's cooling law of Eq. (10)
k_2	stiffness coefficient
$M(t)$	moment acting on the shaft
M_*	$= \max[M(t)]$; maximum moment acting on the shaft
$M_t(t)$	moment of friction
$M_s(t)$	moment of elastic forces
m_0	dimensionless coefficient in the shaft equation of motion (26)
$N(t)$	normal reaction
$p(\tau)$	dimensionless contact pressure
p_{st}	dimensionless steady-state contact pressure
$P(t)$	contact pressure
P_*	characteristic contact pressure value for nonmovable system while the shaft is heated to temperature T_*
r	dimensionless radius
R	radius
R_1, R_2	internal and external radii of the bush, respectively
s	Laplace transform parameter
t	time
t_D	$= \sqrt{B_2/k_2}/R_2$; characteristic system time related to the bush oscillations period
t_T	$= R_1^2/a_1$; characteristic time related to heat transfer
T	period of oscillation
$T_1(R, t)$	temperature of the shaft
T_*	maximal environment temperature
$U(X, t)$	displacement component along radial direction in the shaft
$V_r(t)$	relative velocity of the shaft and the bush
V_*	$= R_1/t_T$; characteristic velocity
v	dimensionless coefficient related to frictional TEI
α_1	coefficient of thermal expansion of the shaft
α_T	heat transfer coefficient
β_1, β_2	dimensionless coefficient related to friction and its derivative
γ	dimensionless thermomechanical parameter in the boundary conditions (18)
$\theta(r, \tau)$	dimensionless temperature of the shaft
θ_{st}	dimensionless steady-state contact temperature
$\varepsilon_1, \varepsilon_2$	dimensionless coefficients related to moment of shaft and bush inertia, respectively [see Eqs. (26) and (5)]
ν	Poisson's ratio of the shaft
$\varphi(\tau)$	dimensionless shaft position angle
$\varphi_1(t), \varphi_2(t)$	angles of the shaft and the bush position, respectively
λ_1	thermal conductivity of the shaft
$\sigma_R(R, t)$	stress component along radial direction in the shaft
$\tilde{\omega}$	t_D/t_T; coupling parameter of the system
ω_{st}	dimensionless steady-state shaft angular velocity
τ	dimensionless time
$\phi(\tau)$	dimensionless shaft position angle

their occurrence and behavior of the contact characteristics (relative velocity, contact temperature, and contact pressure) may lead to a better understanding and explanation of various complex processes in friction brakes, grinding machines, machine tools (where high-accuracy treatment is required), in torsional joints, various frictional dampers, as well as in other machine systems with friction kinematic pairs.

The classical problem devoted to the analysis of a friction pad on a rotating shaft, which is fixed elastically to a housing (massless springs), was investigated in monographs [2, 8]. Constant velocity for shaft rotation has been assumed by Andronov et al. [2], and the shaft inertia were included by Neimark [8]. In fact, this simple model corresponds to a typical braking pad model or to Prony's clamp model [2]. Both fast and slow pad movements were analyzed under the assumption that the mass of the pad tends to zero.

A thermoelastic contact between a rotating shaft and a fixed pad was investigated by Pyryev and co-workers [10, 11], under the assumption that the contact is non-inertial. A dynamical problem of the thermoelastic contact with the frictional heating of the contacting surfaces was studied in the literature [11–16]. The axially symmetric problem of the thermoelastic contact of a shaft that rotates with constant velocity (later referred to as the kinematic excitation) and a pad fixed to the housing via massless springs was analyzed by Awrejcewicz and Pyryev [17] and, with wear and frictional heat generation taken into account, self-excited vibrations caused by friction were examined. It was also shown that when the relative speed achieves its critical value, the so-called frictional thermoelastic instability (TEI) occurs.

The present work is a continuation of the problem considered by Awrejcewicz and Pyryev [17]. Here, a more complicated case is studied, namely the one in which one of the contacting bodies is subjected to mechanical excitation and, hence, an equation governing its dynamics must be included in the full mathematical model of the problem. Many important questions concerning the system under investigation may be formulated. Does frictional TEI occur in this case, and if not, then how is the system dynamics realized? Is it possible to realize a self-excited motion? What kind of system motion appears during the braking process? The answers to these questions are given in this paper. It should also be emphasized that the mechanism for the contact between two bodies dealt with in the present analysis is different from the one discussed in the literature [17].

Observe that the system under analysis is described by two characteristic times, namely, the characteristic time related to system oscillations, t_D (small), and the characteristic time related to heat transfer, t_T (large). If the ratio of these two timescales is "small," then the system can be treated as an uncoupled one.

Numerical verification of the presented analytical estimations of periodic oscillations completes the paper.

THE SYSTEM UNDER ANALYSIS

An elastic and heat-transferring shaft of radius R_1 has been inserted into a bush (solid bearing bushing or a braking pad) of external radius R_2 and internal radius R_1. The diagram of the analyzed system is shown in Figure 1. The bush is attached to the housing (a frame or a base) through springs characterized by stiffness coefficient k_2. It is assumed that the bush behaves like a rigid body. The shaft rotates with angular velocity $\dot{\varphi}_1(t)$, and the centrifugal forces are neglected. The angular velocity of the shaft is assumed to change due to the action of the moment $M = M_* h_M(t)$, where M_* is a constant, and $h_M(t)$ is a known dimensionless function of time ($h_M(t) \to 1, t \to \infty$).

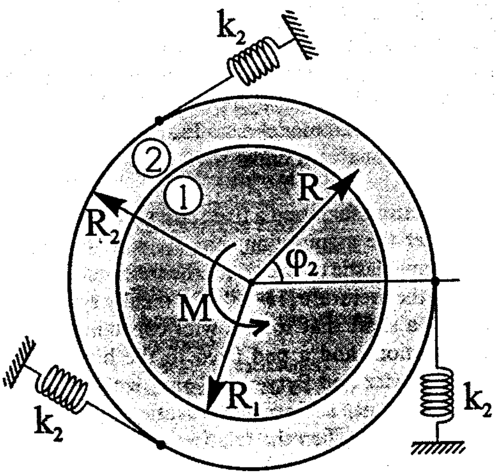

Figure 1. The analyzed system.

It is further assumed that the bush transfers heat ideally and that at the initial time instant the ambient temperature change is governed by $T_* h_T(t)$, where T_* is a constant in temperature units, while $h_T(t)$ stands for a known dimensionless function of time ($h_T(t) \to 1$, $t \to \infty$), and that between the shaft and the bush the Newton heat exchange occurs. The shaft starts to expand, and a contact between the shaft and the bush is initiated. Another assumption made is that the dry friction occurring between the bush and the shaft is defined by the function $F_t(V_r)$, where $V_r = \dot{\varphi}_1 R_1 - \dot{\varphi}_2 R_1$ is the relative velocity of the shaft and the bush. Moreover, B_1 and B_2 are moments of inertia of the shaft and the bush, respectively, and the friction force F_t is represented by $F_t = f(V_r)N(t)$, where $N(t)$ is the normal reaction and $f(V_r)$ is a friction coefficient. The friction coefficient is defined as

$$f(V_r) = \mathrm{sgn}(V_r)\begin{cases} f_k(V_r) & \text{if } |V_r| > 0 \\ f_s & \text{if } V_r = 0 \end{cases}, \qquad \mathrm{sgn}(V_r) = \begin{cases} \{V_r/|V_r|\} & \text{if } V_r \neq 0 \\ [-1, 1] & \text{if } V_r = 0 \end{cases}$$

where f_s stands for the maximum value of the static friction coefficient and $f_k(V_r)$ denotes the kinetic friction coefficient. The so-called Stribeck curve [4,6], shown in Figure 2, has its minimum for $V_r = V_{\min}$, and for $V_r < V_{\min}$ we have $f_k'(V_r) < 0$. The friction force F_t yields heat generated by friction on the contact surface $R = R_1$. Observe that the frictional work is transformed to heat energy (see, for instance [18]). Let the shaft temperature, denoted by $T_1(R, t)$, be initially equal to zero.

The formulated problem is defined by the equations that govern the dynamics of the bodies in the vicinity of the equilibrium configuration, with angular displacements $\varphi_2(t)$ and $\varphi_1(t)$, and angular velocities $\dot{\varphi}_2(t)$ and $\dot{\varphi}_1(t)$, respectively for the bush and the shaft, with stress $\sigma_R(R, t)$ in the shaft, contact pressure

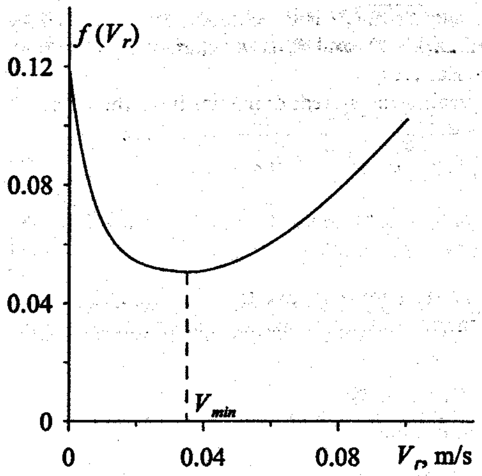

Figure 2. Kinetic friction coefficient versus relative velocity.

$P(t) = N(t)/2\pi R_1 = -\sigma_R(R_1, t)$, temperature $T_1(R, t)$ of the shaft, and with the linear displacement $U(R, t)$ in the direction along axis R.

MATHEMATICAL FORMULATION OF THE PROBLEM

Equations for Rotational Movement of Rigid Bush

Let axis Z be the cylinder axis. The equilibrium state of the moments of forces with respect to the shaft axis yields (cf. [3, 17])

$$B_2\ddot{\varphi}_2 - M_s = M_t \tag{1}$$

where $M_t = f(R_1(\dot{\varphi}_1 - \dot{\varphi}_2))2\pi R_1^2 P(t)$ denotes the moment of friction force and $M_s = k_2 R_2^2 \varphi_2$ is the moment of the elastic forces.

Let the initial conditions be

$$\varphi_2(0) = \varphi_2^\circ, \qquad \dot{\varphi}_2(0) = \omega_2^\circ \tag{2}$$

and let us introduce the dimensionless parameters

$$\tau = \frac{t}{t_T} \qquad p = \frac{P}{P_*} \qquad \varepsilon_2 = \frac{2\pi R_1^2 t_T^2 P_*}{B_2} \qquad \tilde{\omega} = \frac{t_D}{t_T}$$
$$\varphi^\circ = \varphi_2^\circ \qquad \omega^\circ = t_T\omega_2^\circ \qquad \varphi(\tau) = \varphi_2(t_T\tau) \tag{3}$$

$$F(\dot{\phi} - \dot{\varphi}) = f(V_*(\dot{\phi} - \dot{\varphi})) \tag{4}$$

where τ is the dimensionless time, $t_D = \sqrt{B_2/k_s}/R_2$ is the characteristic system time related to the bush oscillations period $2\pi t_D = T$, and P_* is the characteristic contact pressure at shaft temperature T_* [see Eq. (16)].

The dimensionless equations governing the system dynamics have the form

$$\ddot{\varphi}(\tau) + \tilde{\omega}^{-2}\varphi(\tau) = \varepsilon_2 F(\dot{\phi} - \dot{\varphi})p(\tau), \qquad 0 < \tau < \infty \tag{5}$$

$$\varphi(0) = \varphi^\circ \qquad \dot{\varphi}(0) = \omega^\circ \tag{6}$$

To solve the motion equations one needs to know $\dot{\varphi}(\tau)$ and the contact pressure $p(\tau)$. The latter can be obtained from the thermoelasticity equation that includes also the tribological processes.

Problem Formulation for Thermoelastic Shaft

In the analyzed case, the inertial terms in the equation of motion can be omitted and the problem may be considered a quasi-static one. For the axially symmetric stress of the shaft, the equations used belong to the theory of thermal stresses for an isotropic body, stated by Nowacki [19] and applying cylindrical coordinates (R, ϕ, Z):

$$\frac{\partial^2 U(R,t)}{\partial R^2} + \frac{1}{R}\frac{\partial U(R,t)}{\partial R} - \frac{1}{R^2}U(R,t) = \alpha_1 \frac{1+\nu}{1-\nu}\frac{\partial T_1(R,t)}{\partial R} \tag{7}$$

$$\frac{\partial^2 T_1(R,t)}{\partial R^2} + \frac{1}{R}\frac{\partial T_1(R,t)}{\partial R} = \frac{1}{a_1}\frac{\partial T_1(R,t)}{\partial t} \qquad 0 < R < R_1 \qquad 0 < t < \infty \tag{8}$$

with mechanical boundary conditions

$$U(0,t) = 0 \qquad U(R_1,t) = 0 \qquad 0 < t < \infty \tag{9}$$

thermal boundary conditions

$$\lambda_1 \frac{\partial T_1(R_1,t)}{\partial R} + \alpha_T(T_1(R_1,t) - T_* h_T(t)) = f(V_r)V_r P(t) \tag{10}$$

$$R\frac{\partial T_1(R,t)}{\partial R}\bigg|_{R\to 0} = 0 \qquad 0 < t < \infty \tag{11}$$

and with the initial condition

$$T_1(R,0) = 0 \qquad 0 < R < R_1 \tag{12}$$

Radial stress $\sigma_R(R,t)$ in the cylinder may be found with the use of radial displacement $U(R,t)$ and temperature $T_1(R,t)$ by the application of the formula

$$\sigma_R(R,t) = \frac{E_1}{1-2\nu}\left[\frac{1-\nu}{1+\nu}\frac{\partial U(R,t)}{\partial R} + \frac{\nu}{1+\nu}\frac{U(R,t)}{R} - \alpha_1 T_1(R,t)\right] \tag{13}$$

The following notation is used: $P(t) = N(t)/2\pi R_1 = -\sigma_R(R_1,t)$ denotes contact pressure, and $h_T(t)$ denotes environment temperature for the Newton cooling law in Eq. (10).

Integration equation (7), with Eqs. (9) and (13) taken into account, leads to determination of the contact pressure:

$$P(t) = \frac{2E_1\alpha_1}{1-2\nu}\frac{1}{R_1^2}\int_0^{R_1} T_1(\xi,t)\xi d\xi \tag{14}$$

Let us introduce the following dimensionless parameters:

$$r = \frac{R}{R_1} \qquad u = \frac{U}{\alpha_1 T_*(1+\nu)R_1} \qquad \theta = \frac{T_1}{T_*}$$
$$Bi = \frac{\alpha_T R_1}{\lambda_1} \qquad h_T(\tau) = h_T(t_T\tau) \qquad \gamma = \frac{E_1\alpha_1 a_1}{(1-2\nu)\lambda_1} \tag{15}$$

where

$$P_* = E_1\alpha_1 T_*/(1-2\nu) \qquad t_T = \frac{R_1^2}{a_1} \tag{16}$$

and t_T is the characteristic time of the thermal inertia. Observe that parameter γ is proportional to the parameter$\delta_1 = \alpha_1(1+\nu)/\lambda_1$ (where δ_1 is the thermal distortivity) known in the literature (see, for example, [1]).

The thermoelastic problem under consideration takes the following dimensionless form:

$$\frac{\partial^2\theta(r,\tau)}{\partial r^2} + \frac{1}{r}\frac{\partial\theta(r,\tau)}{\partial r} = \frac{\partial\theta(r,\tau)}{\partial\tau} \qquad 0<\tau<\infty \qquad 0<r<1 \tag{17}$$

$$\frac{\partial\theta(1,\tau)}{\partial r} + Bi(\theta(1,\tau) - h_T(\tau)) = \gamma F\left(\dot\phi(\tau) - \dot\varphi(\tau)\right)\left(\dot\phi(\tau) - \dot\varphi(\tau)\right)p(\tau) \qquad 0<\tau<\infty \tag{18}$$

$$r\frac{\partial\theta(r,\tau)}{\partial r}\bigg|_{r\to 0}=0 \qquad 0<\tau<\infty \tag{19}$$

$$\theta(r,0)=0 \qquad 0<r<1 \tag{20}$$

$$p(\tau)=2\int_0^1 \theta(\xi,\tau)\xi d\xi \qquad 0<\tau<\infty \tag{21}$$

The radial displacement is defined by

$$u(r,\tau)/r=\frac{1}{(1-\nu)}\left[\frac{1}{r^2}\int_0^r \theta(\eta,\tau)\eta d\eta-\int_0^1 \theta(\eta,t)\eta d\eta\right] \tag{22}$$

Observe that in order to solve the problem defined by Eqs. (17)–(22) one should know the time-dependent velocities of the bush and the shaft. Notice also that problems (5),(6), and (17)–(22) are mutually adjoint and require simultaneous solving.

Equations for Rotational Motion of the Shaft

Let axis Z coincide with the shaft axis. The force moments related to the shaft axis give [3]

$$B_1\ddot{\varphi}_1-M=-M_t \tag{23}$$

where $M_t=f(V_r)2\pi R_1^2P(t)$ denotes moment of friction force, M is the moment acting on the shaft, and $\varphi_1(t)$ stands for the angle of the shaft position. In order to solve Eq. (23) the following initial conditions are used:

$$\varphi_1(0)=\varphi_1^\circ \qquad \dot{\varphi}_1(0)=\omega_1^\circ \tag{24}$$

Introducing the dimensionless parameters

$$\varepsilon_1=\frac{2\pi R_1^2t_T^2P_*}{B_1} \qquad m_0=\frac{M_*}{P_*2\pi R_1^2} \qquad \phi^\circ=\varphi_1^\circ \qquad \dot{\phi}^\circ=t_T\omega_1^\circ \qquad \phi=\varphi_1(t_T\tau)$$

$$h_M(\tau)=h_M(t_T\tau) \qquad F(\dot{\phi}-\dot{\varphi})=f(V_*(\dot{\phi}-\dot{\varphi})) \tag{25}$$

one gets the dimensionless equation governing the dynamics of the shaft:

$$\ddot{\phi}(\tau)-\varepsilon_1m_0h_M(\tau)=-\varepsilon_1F(\dot{\phi}-\dot{\varphi})p(\tau) \qquad 0<\tau<\infty \tag{26}$$

$$\phi(0) = \phi^{\circ} \qquad \dot{\phi}(0) = \dot{\phi}^{\circ} \tag{27}$$

It is seen that again contact pressure needs to be defined. It will be found following the solving procedure for the thermoelastic equation that takes into account the tribologic processes. Notice that problems (5), (6), (17)–(22), and (26)–(27) are coupled and require simultaneous solving.

ANALYSIS OF THE INVESTIGATED PROCESS

Let us assume that the relative velocity dependence is approximated by the function [17]

$$f(V_r) = \mathrm{sgn}(V_r)\begin{cases} f_{\min} + (f_s - f_{\min})\exp(-b_1|V_r|) & \text{if } |V_r| < V_{\min} \\ [-f_s; f_s] & \text{if } V_r = 0 \\ f_{\min} + (f_s - f_{\min})\exp(-b_1|V_{\min}|) + \dfrac{b_2 b_3(|V_r| - V_{\min})^2}{1 + b_2(|V_r| - V_{\min})} & \text{if } |V_r| > V_{\min} \end{cases} \tag{28}$$

where $f_s = 0.12$, $f_{\min} = 0.05$, $b_1 = 140\ \mathrm{sm}^{-1}$, $b_2 = 10\ \mathrm{sm}^{-1}$, $b_3 = 2\ \mathrm{sm}^{-1}$, and $V_{\min} = 0.035\ \mathrm{mc}^{-1}$ (see [7]). The function $F(y) = f(V_* y)$ has a local minimum for $y_{\min} = V_{\min}/V_*$. In the numerical analysis, function $\mathrm{sgn}(x)$ is approximated by [5]

$$\mathrm{sgn}_{\varepsilon_0}(x) = \begin{cases} 1 & \text{if} > \varepsilon_0 \\ \left(2 - \dfrac{|x|}{\varepsilon_0}\right)\dfrac{x}{\varepsilon_0} & \text{if } |x| < \varepsilon_0 \\ -1 & \text{if } x < -\varepsilon_0 \end{cases} \tag{29}$$

where $\varepsilon_0 = 0.0001$.

Laplace Transformation Method

Let us apply the Laplace transformation to Eqs. (17)–(22):

$$\{\bar{\theta}(r,s), \bar{p}(s), \bar{h}_T(s), \bar{q}(s)\} = \int_0^{\infty} \{\theta(r,\tau), p(\tau), h_T(\tau), q(\tau)\} e^{-s\tau} d\tau$$

where s is the transformation parameter. Taking into account boundary conditions (18) and (19) and initial condition (20) we obtain

$$\bar{\theta}(r,s) = sG_\theta(r,s)\bar{q}(s) \qquad \bar{p}(s) = 2sG_p(s)\bar{q}(s)$$

$$G_\theta(r,s) = \frac{I_0(\sqrt{s}r)}{s\Delta_1(s)} \qquad G_p(s) = \frac{\Delta_2(s)}{s\Delta_1(s)} \tag{30}$$

$$\Delta_2(s) = I_1(\sqrt{s})/\sqrt{s} \qquad \Delta_1(s) = s\Delta_2(s) + BiI_0(\sqrt{s})$$

where $I_n(x) = i^{-n}J_n(ix)$ is a modified Bessel function of the first order with argument x, and the nonlinear part of boundary problem (18) has the form

$$q(\tau) = \gamma F(\dot{\phi} - \dot{\varphi})(\dot{\phi} - \dot{\varphi})p(\tau) + Bi\, h_T(\tau)$$

To determine the inverse Laplace transform one may use well-known methods to find the sums of the residues of the functions $G_\theta(r,s)e^{-s\tau}$ and $G_p(s)e^{-s\tau}$ in the complex plane. Using Eq. (30), applying the inverse Laplace transform, and using the theorem of convolution [20], the following functions are found:

$$p(\tau) = 2Bi\int_0^\tau G_p(\tau-\xi)\dot{h}_T(\xi)d\xi + 2\gamma\int_0^\tau \dot{G}_p(\tau-\xi)F(\dot{\phi}-\dot{\varphi})p(\xi)(\dot{\phi}-\dot{\varphi})d\xi \qquad (31)$$

$$\theta(r,\tau) = Bi\int_0^\tau G_\theta(r,\tau-\xi)\dot{h}_T(\xi)d\xi + \gamma\int_0^\tau \dot{G}_\theta(r,\tau-\xi)F(\dot{\phi}-\dot{\varphi})p(\xi)(\dot{\phi}-\dot{\varphi})d\xi \qquad (32)$$

where

$$\{G_p(\tau), G_\theta(1,\tau)\} = \frac{\{0.5, 1\}}{Bi} - \sum_{m=1}^{\infty}\frac{\{2Bi, 2\mu_m^2\}}{\mu_m^2(Bi^2+\mu_m^2)}e^{-\mu_m^2\tau} \qquad (33)$$

and $\mu_m (m = 1, 2, 3, \ldots)$ are the roots of the characteristic equation

$$BiJ_0(\mu) - \mu J_1(\mu) = 0 \qquad (34)$$

Notice that the investigated problem has been transformed to the set of nonlinear differential equations (5) and (26), integral equation (31) describing angular velocities $\dot{\varphi}(\tau)$ and $\dot{\phi}(\tau)$, and contact pressure $p(\tau)$. The temperature is defined by Eqs. (32) and (33).

To sum up, on introducing boundary condition (18) one arrives at a coupled problem of two-degree-of-freedom oscillations and a thermoelastic problem of the rotating shaft. For $\gamma = 0$ (no frictional heat generation), the contact pressure $p(\tau) \to 1$, and the system of equations (5) and (26) that governs the coupled oscillations in the shaft bushing system is obtained. Note that owing to the increase of the spring stiffness ($k_2 \to \infty$) the characteristic time $t_D \to 0$, which yields $\tilde{\omega} \to 0$ and $\varphi \to 0$. The obtained Eqs. (26), (31), and (32) govern the contact problem of the rotating thermoelastic shaft. The natural question that arises is how to define the key control parameters γ and $\tilde{\omega}$ for the system which is either coupled or uncoupled. This question is addressed in a future study.

Steady-State Solution Analysis

Observe that, in Eq. (26), the variable $\phi(\tau)$ does not appear and, hence, the phase space of the bush–shaft system is three-dimensional [8]. Consider the case when after a transitional process the cylinder starts to rotate with constant velocity $\dot{\phi}(\tau) = \omega_{st}$ while the bush does not move, $\dot{\varphi} = 0$. Then, the steady-state solution of the problem under consideration (in Eq. (17) the differential terms are omitted) has the following form:

$$p_{st} = \frac{1}{1-v} = \frac{m_0}{F(\omega_{st})} \qquad \theta_{st} = \frac{1}{1-v} \qquad \varphi_{st} = \tilde{\omega}^2 \varepsilon_2 F(\omega_{st}) p_{st} = \tilde{\omega}^2 \varepsilon_2 m_0$$
$$v = \frac{\gamma \omega_{st} F(\omega_{st})}{Bi} \tag{35}$$

where ω_{st} is a solution to the nonlinear equation

$$F(\omega_{st}) = \frac{m_0}{1 + \gamma m_0 \omega_{st}/Bi} \tag{36}$$

In the preceding equations, m_0 is an applied dimensionless moment, γ is a parameter related to thermal distortivity, and Bi is the Biot number.

In Figure 3, the graphical solution of Eq. (36) for various parameters m_0 and Bi is shown. For a stainless steel shaft ($\alpha_1 = 14 \times 10^{-6}{}^\circ\text{C}^{-1}$, $\lambda_1 = 21\text{Wm}^{-1}{}^\circ\text{C}^{-1}$, $\nu = 0.3$, $a_1 = 5.9\ \text{mm}^2\text{s}^{-1}$, $E_1 = 190$ GPa) parameter $\gamma = 1.87$, and for $R_1 = 4 \times 10^{-3}$ m the characteristic time $t_T = 2.71$ s, and $V_* = 1.47 \cdot 10^{-3}\ \text{ms}^{-1}$. Solid curve 1 corresponds to $m_0 = 0.14$, $Bi = 10$; solid curve 2 corresponds to $m_0 = 0.1$, $Bi = 10$; solid curve 3 corresponds to $m_0 = 0.05$, $Bi = 10$; and solid curve 4 corresponds to $m_0 = 0.14$, $Bi = 1$. The dashed curve represents function $F(\omega_{st})$.

Equation (36) may have one solution ω_{st}^3 ($F'(\omega_{st}^3) > 0$) for $m_0 = 0.14$, $Bi = 10$ (first case); three solutions ω_{st}^1, ω_{st}^2, ω_{st}^3 ($F'(\omega_{st}^1) > 0, F'(\omega_{st}^2) < 0, F'(\omega_{st}^3) > 0$) for $m_0 = 0.1$, $Bi = 10$ (second case); one solution $\omega_{st}^1 = 0$ for $m_0 = 0.05$, $Bi = 10$ and for approximation (29) $\omega_{st}^1 \approx \varepsilon_0 m_0/2f_s$, $F'(\omega_{st}^1) \approx 2f_s/\varepsilon_0$ (third case); or one solution ω_{st}^2 ($F'(\omega_{st}^2) < 0$) for $m_0 = 0.14$, $Bi = 1$ (fourth case). For a small value of γ/Bi ($\gamma/Bi << 1$) (frictional heat generation is neglected, $\gamma = 0$) and for $m_0 \in [0, f_{\min})$, Eq. (36) can have one solution $\omega_{st}^1 = 0$. It may also have three solutions ω_{st}^1, ω_{st}^2, and ω_{st}^3, for $m_0 \in (f_{\min}, f_s)$, and one solution ω_{st}^3 for $m_0 \in (f_s, \infty)$. Equation (36) shows that the stationary solution does not depend on parameter $\tilde{\omega}$. Let us now analyze perturbations of stationary process (35), which are defined by the equation $h_T(\tau) = 1 + h_T^*(\tau)$.

A solution is sought in the form

$$\varphi(\tau) = \varphi_{st} + \varphi^*(\tau) \qquad \theta(r,\tau) = \theta_{st}(r) + \theta^*(r,\tau) \qquad p(\tau) = p_{st} + p^*(\tau)$$

$$\dot{\varphi} = \dot{\varphi}^*(\tau) \qquad \dot{\phi} = \omega_{st} + \dot{\phi}^*(\tau)$$

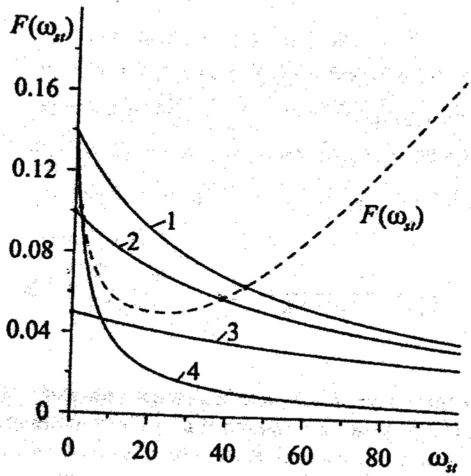

Figure 3. Graphical solution to Eq. (36). Solid curves: 1, $m_0 = 0.14$, $Bi = 10$; 2, $m_0 = 0.1$, $Bi = 10$; 3, $m_0 = 0.05$, $Bi = 10$; 4, $m_0 = 0.14$, $Bi = 1$. Dashed curve corresponds to $F(\omega_{st})$.

where

$$|\varphi^*| << 1 \qquad |\theta^*| << 1 \qquad |p^*| << 1 \qquad |\dot\varphi^*| << 1 \qquad |\dot\phi^*| << 1$$

After linearization of the right-hand sides of Eqs. (5), (26), and boundary condition (18), the following set of perturbation equations is obtained:

$$\ddot\varphi^*(t) + \tilde\omega^{-2}\varphi^*(t) = \varepsilon_2 F(\omega_{st})p^*(\tau) + \varepsilon_2 F'(\omega_{st})p_{st}(\dot\phi^* - \dot\varphi^*) \qquad 0 < \tau < \infty \tag{37}$$

$$\varphi^*(0) = 0 \qquad \dot\varphi^*(0) = 0 \tag{38}$$

$$p^*(\tau) = 2\int_0^1 \theta^*(\xi,\tau)\xi d\xi \qquad 0 < \tau < \infty \tag{39}$$

$$\frac{\partial^2\theta^*(r,\tau)}{\partial r^2} + \frac{1}{r}\frac{\partial\theta^*(r,\tau)}{\partial r} = \frac{\partial\theta^*(r,\tau)}{\partial\tau} \qquad 0 < \tau < \infty \qquad 0 < r < 1 \tag{40}$$

$$\frac{\partial\theta^*(1,\tau)}{\partial r} + Bi\theta^*(1,\tau) = Bih_T^* + \gamma\Big[\omega_{st}F(\omega_{st})p^*(\tau) + p_{st}(\dot\phi^* - \dot\varphi^*)(F(\omega_{st}) + \omega_{st}F'(\omega_{st}))\Big] \tag{41}$$

$$r\frac{\partial\theta^*(r,\tau)}{\partial r}\bigg|_{r\to 0}=0 \qquad 0<\tau<\infty \qquad \theta^*(r,0)=0 \qquad 0<r<1 \tag{42}$$

$$\ddot{\phi}^*(t)=-\varepsilon_1\left[F(\omega_{st})p^*+F'(\omega_{st})p_{st}(\dot{\phi}^*-\dot{\varphi}^*)\right] \qquad 0<\tau<\infty \tag{43}$$

$$\phi^*(0)=0 \qquad \dot{\phi}^*(0)=0 \tag{44}$$

Application of the Laplace transformation to the linear system (37)–(44) of the form

$$\{\bar{\theta}^*(r,s),\bar{p}^*(s),\bar{\varphi}^*(s),\bar{h}_T^*(s),\bar{\phi}^*(s)\}=\int_0^\infty\{\theta^*,p^*,\varphi^*,h_T^*,\phi^*\}e^{-s\tau}d\tau$$

yields a solution in the Laplace transform domain. The characteristic equation of the linearized problem is of the form

$$\Delta_1^*(s)=0 \tag{45}$$

$$\Delta_1^*(s)=s\Delta^*(s)+\varepsilon_1 p_{st}(\bar{\omega}^2 s^2+1)[\beta_2\Delta_1(s)+2Biv\beta_1\Delta_2(s)]$$

$$\Delta^*(s)=\Delta_1(s)\Omega_2(s)-2Biv\Delta_2(s)\Omega_1(s) \tag{46}$$

$$\Omega_1(s)=\bar{\omega}^2(s^2-\varepsilon_2 p_{st}\beta_1 s)+1 \qquad \Omega_2(s)=\bar{\omega}^2(s^2+\varepsilon_2 p_{st}\beta_2 s)+1$$
$$\beta_2=F'(\omega_{st}) \qquad \beta_1=F(\omega_{st})\omega_{st}$$

The roots s_m ($\mathrm{Re}s_1>\mathrm{Re}s_2>\cdots>\mathrm{Re}s_m>\cdots, m=1,2,3,\ldots$) of characteristic equation (45) may lie in the left-hand part (LHP) $\mathrm{Re}s<0$ (a stationary solution is stable) or in the right-hand part (RHP) $\mathrm{Re}s>0$ (a stationary solution is unstable) of the complex plane (s is a complex variable). The parameters separating the two half-planes are called critical.

If the frictional heat generation is not taken into account ($\gamma=0$), the characteristic equation is governed by the following cubic equation: $s\Omega_2(s)+\beta_2\varepsilon_1(\bar{\omega}^2s^2+1)=0$. Its roots lie in the RHP of the complex plane if $\beta_2<0$. For a given bush velocity (one may assume $\varepsilon_1\to 0$), the characteristic equation is reduced to the form $\Delta^*(s)=0$ (for more details see [17]), whereas for $\gamma=0$ (that is, when the frictional heat generation is not taken into account) it reads $\Omega_2(s)=0$.

Let us analyze the stationary stable solution in more detail. The characteristic function has the form

$$\Delta_1^*(s)=\sum_{m=0}^{\infty}s^m b_m \tag{47}$$

$$b_0 = \varepsilon_1 B_i p_{st}(\beta_2 + v\beta_1) \quad d_0 = Bi(1-v)$$
$$b_1 = d_0 + \varepsilon_1 p_{st}[2(2+B_i)\beta_2 + Biv\beta_1]/8$$
$$d_1 = 0.5 + Bi[0.25 - 0.125v + \tilde{\omega}^2 p_{st}\varepsilon_2(\beta_2 + v\beta_1)]$$
$$b_m = d_{m-1} + \varepsilon_1 p_{st}[(d_m^{(1)} + \tilde{\omega}^2 d_{m-2}^{(1)})\beta_2 + 2Biv(d_m^{(2)} + \tilde{\omega}^2 d_{m-2}^{(2)})\beta_1]$$
$$d_m = d_m^{(1)} - 2Bivd_m^{(2)} + \tilde{\omega}^2\varepsilon_2 p_{st}\left(\beta_2 d_{m-1}^{(1)} + 2Biv\beta_1 d_{m-1}^{(2)}\right) + \tilde{\omega}^2\left(d_{m-2}^{(1)} - 2Bivd_{m-2}^{(2)}\right)$$
$$m = 2, 3, \ldots$$
$$d_m^{(1)} = \frac{Bi + 2m}{2^{2m}(m!)^2} \qquad d_m^{(2)} = \frac{1}{2^{2m+1}m!(1+m)!} \qquad m = 0, 1, \ldots$$

It should be emphasized that, for a given shaft velocity ($\varepsilon_1 \to 0$), Eq. (47) yields the condition $v > 1$ of a frictional TEI (see [17]). However, when the moment of inertia of the shaft ($\varepsilon_1 > 0$) is taken into account, then the frictional TEI does not occur. In the latter case, the system self-controls the rotational shaft velocity by keeping always $v < 1$. Note that the shaft dynamics influences significantly the values of the characteristic equation roots only if the parameter $\tilde{\omega}^2(\varepsilon_2 + \varepsilon_2)$ cannot be considered a "small" one.

Under the assumption of the temperature increase of the surrounding medium by up to $T_* = 5°C$ the stainless steel shaft of radius $R_1 = 4 \cdot 10^{-3}$ m is further investigated ($P_* = 33.2$ MPa and $t_T = 2.71$ s). Furthermore, it is assumed that either the moment $M_* = 334$ N ($m_0 = 0.1$) or the moment $M_* = 468$ N ($m_0 = 0.14$) is applied to the shaft. Let either $\alpha_T = 5.25 \times 10^4\,\mathrm{Wm^{-2}{}^\circ C^{-1}}$ ($Bi = 10$) or $\alpha_T = 5.25 \times 10^3\,\mathrm{Wm^{-2}{}^\circ C^{-1}}$ ($Bi = 1$). It is also assumed that the shaft moment of inertia $B_1 = 245.8$ kg · m ($\varepsilon_1 = 100$). On the other hand, it is assumed that the bush moment of inertia $B_2 = 245.8$ kg · m (the external radius $R_2 = 4 \times 10^{-2}$ m), and the stiffness of the springs $k_2 = 2.1 \times 10^6\,\mathrm{N/m^2}$ (which yields $t_D = 0.271$ s and $\varepsilon_2 = 100$). The ratio of small t_D and large t_T timescales reads $\tilde{\omega} = 0.1$.

In the first case ($m_0 = 0.14$, $Bi = 10$) there is one solution $\omega_{st}^3 = 44.40$, $p_{st}^3 = \theta_{st}^3 = 2.16$, $\varphi_{st}^3 = 0.14$ ($\beta_1 = 0.14 \times 10^{-2}$, $\beta_2 = 0.12 \times 10^{-2}$, $v = 0.54$), which is stable [the first roots of Eq. (45), $s_{1,2} = -0.18 \pm 10.07i$, lie in the LHP]. The expected "period" of damped oscillations is equal to $2\pi/\mathrm{Im}s_1 = 0.62$.

In the second case ($m_0 = 0.1$, $Bi = 10$), there are three solutions. The solution $\omega_{st}^3 = 38.40$, $p_{st}^3 = \theta_{st}^3 = 1.72$, $\varphi_{st}^3 = 0.1$ ($\beta_1 = 0.15 \times 10^{-2}$, $\beta_2 = 0.1 \times 10^{-2}$, $v = 0.41$) is stable [the first roots of Eq. (45), $s_{1,2} = -0.11 \pm 10.04i$, $s_3 = -0.53$, lie in the LHP). The solution $\omega_{st}^2 = 1.99$ ($\beta_1 = 4.85 \times 10^{-2}$, $\beta_2 = -0.96 \times 10^{-2}$, $v = 3.58 \cdot 10^{-2}$) is unstable [the roots of Eq. (45), $s_{1,2} = 0.47 \pm 9.97i$, $s_3 = 0.87$, lie in the RHP]. The solution with approximation (29), $\omega_{st}^1 = 0.42 \times 10^{-4}$ ($\beta_1 = 2.4 \times 10^3$, $\beta_2 = 2.4 \times 10^3$, $v = 7.8 \cdot 10^{-7}$) corresponds to a periodic motion when the bush and shaft stick together ($\omega_{st}^1 \approx 0$) [the roots of Eq. (45) $s_{1,2} = -0.52 \times 10^{-4} \pm 7.07i$ lie on the imaginary axis]. Observe that in the last case the roots may be found directly from the characteristic equation $s^2 + \omega_0^2 = 0$, where $\omega_0 = 1/(\tilde{\omega}\sqrt{1 + \varepsilon_2/\varepsilon_1})$.

In the third case ($m_0 = 0.05$, $Bi = 10$), there is one solution. The solution with approximation (29), $\omega_{st}^1 = 0.21 \times 10^{-4}$, $p_{st}^1 = \theta_{st}^1 = 1.0$, $\varphi_{st}^1 = 0.05$ ($\beta_1 = 2.4 \times 10^3$,

$\beta_2 = 2.4 \times 10^3$, $v = 1.95 \cdot 10^{-7}$), corresponds to a periodic motion [the roots of Eq. (45), $s_{1,2} = -0.52 \times 10^{-4} \pm 7.07i$, are purely imaginary]. Like in the second case, in the case considered now the roots may also be found directly from the characteristic equation $s^2 + \omega_0^2 = 0$.

The steady-state solutions ω_{st}^1 correspond to stick conditions with rigid-body torsional vibrations. The eigenvalues obtained in these cases have a small real part due to regularization of the step function in the Stribeck approximation. These real parts are spurious effects of the regularization and the real physical behavior does not involve any slip.

In the fourth case ($m_0 = 0.14$, $Bi = 1$), there is again only one solution. The solution $\omega_{st}^2 = 1.41$, $p_{st}^2 = \theta_{st}^2 = 1.37$, $\varphi_{st}^2 = 0.14$ ($\beta_1 = 7.28 \times 10^{-2}$, $\beta_2 = -1.08 \times 10^{-2}$, $v = 0.27$) is unstable (the roots of Eq. (45), $s_{1,2} = 0.745 \pm 10.06i$, $s_{3,4} = 0.13 \pm 1.36i$, lie in the RHP). Observe that the roots $s_{1,2}$ crucially affect the self-excited oscillations because they have the largest real parts and yield the oscillations with the estimated period of $T = 2\pi/\mathrm{Im}s_1 = 0.62$, which has been successfully verified numerically. If there exists one unstable solution, then the corresponding unsteady-state solution approaches a "stick-slip" periodic solution.

The most interesting fourth case is characterized by the following limiting cases. For $m_0 = 0.14$, $Bi = 1$, and when the bush vibrations $\tilde{\omega} = 0$ (fifth case) are neglected, only one solution occurs. The solution $\omega_{st}^2 = 1.41$, $p_{st}^2 = \theta_{st}^2 = 1.37$, $\varphi_{st}^2 = 0.14$ ($\beta_1 = 7.28 \times 10^{-2}$, $\beta_2 = -1.08 \times 10^{-2}$, $v = 0.27$) is unstable [the roots of Eq. (45), $s_{1,2} = 0.145 \pm 1.37i$, lie in the RHP]. Note that the roots $s_{1,2}$ can be well approximated via Eq. (35) by taking into account only three first terms of Eq. (36) ($b_0 = 1.2$, $b_1 = -0.043$, $b_2 = 0.615$, $b_3 = 0.0725$). Again, they govern the self-excited oscillations with the period $T = 2\pi/\mathrm{Im}s_1 = 4.58$.

For $m_0 = 0.14$, $Bi = 1$, and with no frictional heat generation ($\gamma = 0$), there is one solution $\omega_{st}^3 = 86.71$, $p_{st}^3 = \theta_{st}^3 = 1$, $\varphi_{st}^3 = 0.14$ ($\beta_1 = 0.16 \times 10^{-2}$, $\beta_2 = 0.21 \times 10^{-2}$, $v = 0$), which is stable [the first roots of Eq. (45), $s_{1,2} = -0.11 \pm 10.0i$, $s_3 = -0.216$, lie in the LHP). As expected, the motion has the character of damped oscillations with the period $(2\pi/\mathrm{Im}s_1) = 0.629$ and with the logarithmic decrement $(2\pi\mathrm{Re}s_1/\mathrm{Im}s_1) = 0.068$.

When comparing the roots of the last and the first case it becomes clear that if the frictional heat generation ($|\mathrm{Re}s_1|$) is taken into account, then the logarithmic oscillation decrement increases; however, the period of the damped oscillations increases only slightly.

Analysis of the Stick-Slip Process

Let us analyze the system for $t \to \infty$ ($h_M(\tau) = 1$), when a "stick" $\omega_r = \dot{\phi} - \dot{\varphi} = 0$ for $\tau \in t_{st}$ $(t_{st} = (\tau_1, \tau_2) \cup \cdots (\tau_{2i-1}, \tau_{2i}) \cup \cdots)$, or a "slip" for $\tau \in t_{sl}$ $(t_{sl} \in (0, \tau_1) \cup \cdots (\tau_{2i}, \tau_{2i+1}) \cup \cdots)$ occurs. In the first case, $\tau \in t_{st}$, the bush and the cylinder move together, and the governing equation has the form

$$\ddot{\varphi}(\tau) + \omega_0^2 \varphi(\tau) = \varepsilon_2 m_0 \tilde{\omega}^2 \omega_0^2 \qquad \omega_0 = 1/(\tilde{\omega}\sqrt{1 + \varepsilon_2/\varepsilon_1}). \qquad \tau \in t_{st} \qquad (48)$$

The solution of Eqs. (48) describes a periodic motion

$$\varphi(\tau) = \varepsilon_2 m_0 \tilde{\omega}^2 + C_1 \cos(\omega_0 \tau) + C_2 \sin(\omega_0 \tau) \qquad \tau \in t_{st} \tag{49}$$

with the period $2\pi\tilde{\omega}\sqrt{1+\varepsilon_2/\varepsilon_1}$. The cylinder–bush system oscillates periodically, and the bush is subjected to an action of the friction force

$$F(0)p(\tau) = m_0 + \tilde{\omega}^{-2}(C_1 \cos(\omega_0 \tau) + C_2 \sin(\omega_0 \tau))/(\varepsilon_1 + \varepsilon_2) \qquad \tau \in t_{st} \tag{50}$$

The contact pressure is estimated by the formula

$$p(\tau) = 2Bi \int_0^\tau G_p(\tau - \xi)\dot{h}_T(\xi)d\xi + 2\gamma \sum_{m=1}^{i} \int_{\tau_{2m-2}}^{\tau_{2m-1}} \dot{G}_p(\tau - \xi)F(\dot{\phi} - \dot{\varphi})p(\xi)(\dot{\phi} - \dot{\varphi})d\xi$$
$$\tau \in (\tau_{2i}, \tau_{2i+1}) \tag{51}$$

Numerical Analysis

The numerical analysis of the problem was carried out using the Runge–Kutta method for Eqs. (5), (6), (27), and (28), and the quadrature method for Eqs. (31) and (32), applying the asymptotic estimations

$$G_\theta(1,\tau) \approx 2\sqrt{\tau/\pi} \qquad G_p(\tau) \approx \tau \qquad \tau \to 0 \tag{52}$$

Equation (28) was used to approximate the dependence of the friction kinematic coefficient on the relative velocity. Numerical calculations were executed for various values of parameters m_0 and Bi, for which an analytical analysis was performed as well.

Analysis of Acceleration Process ($m_0 > 0$)

Assume that at the initial time instant the force moment $h_M(\tau) = 1 - \exp(-\delta\tau^2)$ acts on the shaft ($\delta = 100$). This force moment causes the shaft to rotate with acceleration. The dimensionless environment temperature is governed by the equation $h_T(\tau) = 1 - \exp(-\delta\tau^2)$. Due to the heat transfer, the rotating cylinder begins to expand and eventually comes into contact with the bush. Figures 4–7 show the outcomes of the calculations carried out for ten values of m_0 and Bi, and for the initial conditions $\varphi^\circ = 0$, $\omega^\circ = 0$, $\phi^\circ = 0$, and $\dot{\phi}^\circ = 0$. Curve 1 illustrates the first case ($m_0 = 0.14$, $Bi = 10$, $\tilde{\omega} = 0.1$, $\gamma = 1.87$), curve 2 represents the second case ($m_0 = 0.1$, $Bi = 10$, $\tilde{\omega} = 0.1$, $\gamma = 1.87$), curve 4 corresponds to fourth case ($m_0 = 0.14$, $Bi = 1$, $\tilde{\omega} = 0.1$, $\gamma = 1.87$), and curve 5 presents the fifth case ($m_0 = 0.14$, $Bi = 1$, $\tilde{\omega} = 0$, $\gamma = 1.87$).

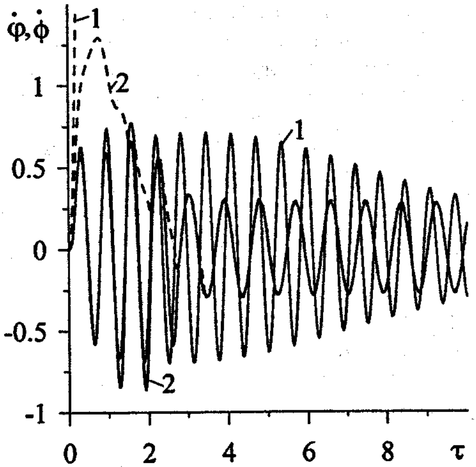

Figure 4. Bush dimensionless velocity $\dot{\varphi}$ (solid curves) and shaft dimensionless velocity $\dot{\phi}$ (dashed curves) versus dimensionless time τ during acceleration for different values of m_0. Curve 1, $m_0 = 0.14$; curve 2, $m_0 = 0.1$.

In Figure 4, the dependence of the dimensionless angular velocity $\dot{\phi}$ of the cylinder (dashed curve) and the bush $\dot{\varphi}$ (solid curve) versus the dimensionless time τ for the first and second of the considered cases is reported. It can be seen that in all cases the system behavior is in agreement with the analytical predictions. In the first case, after certain transitional processes the shaft starts to rotate with constant

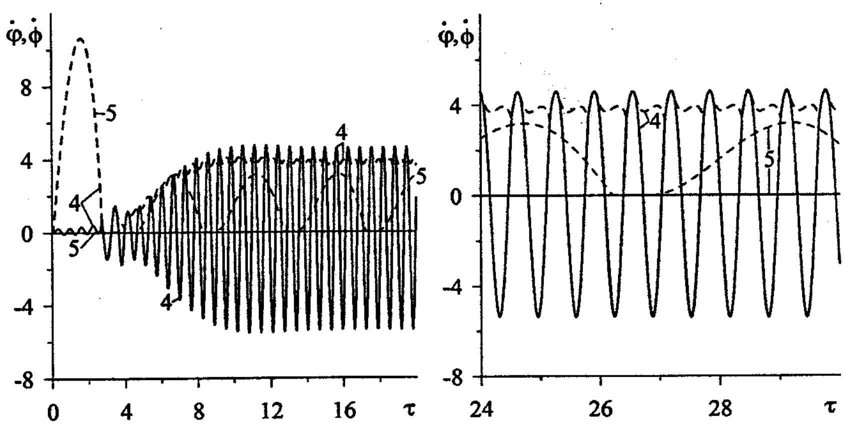

Figure 5. Bush dimensionless velocity $\dot{\varphi}$ (solid curves) and shaft dimensionless velocity $\dot{\phi}$ (dashed curves) versus dimensionless time τ during acceleration for different values of $\bar{\omega}$. Curve 4, $\bar{\omega} = 0.1$; curve 5, $\bar{\omega} = 0$.

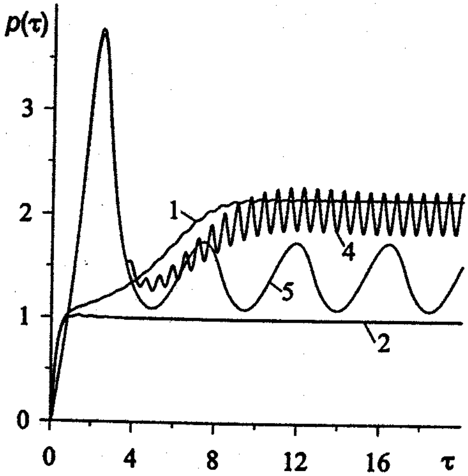

Figure 6. Dimensionless contact pressure p versus dimensionless time τ during acceleration for different values of m_0, Bi, and $\tilde{\omega}$. Curve 1, $m_0 = 0.14$, $Bi = 10$, $\tilde{\omega} = 0.1$; curve 2, $m_0 = 0.1$, $Bi = 10$, $\tilde{\omega} = 0.1$; curve 4, $m_0 = 0.14$, $Bi = 1$, $\tilde{\omega} = 0.1$; curve 5, $m_0 = 0.14$, $Bi = 1$, $\tilde{\omega} = 0$.

velocity $\omega_{st} = 44.4$ The bush displays damped oscillations with the period $T = 0.62$. In the second and third cases (for a small force moment), the cylinder and the bush come into contact and start oscillating periodically as one body with the period $T = 0.89$. The stick-type oscillations are periodic.

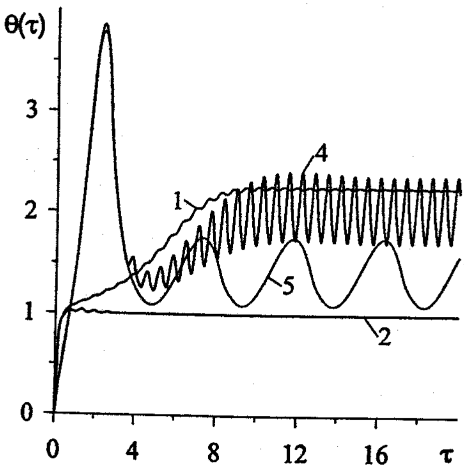

Figure 7. Dimensionless contact temperature $\theta(\tau) = \theta(1, \tau)$ versus dimensionless time τ during acceleration for different values of m_0, Bi, and $\tilde{\omega}$. Curve 1, $m_0 = 0.14$, $Bi = 10$, $\tilde{\omega} = 0.1$; curve 2, $m_0 = 0.1$, $Bi = 10$, $\tilde{\omega} = 0.1$; curve 4, $m_0 = 0.14$, $Bi = 1$, $\tilde{\omega} = 0.1$; curve 5, $m_0 = 0.14$, $Bi = 1$, $\tilde{\omega} = 0$.

In Figure 5, the dependence of the dimensionless angular velocity $\dot{\phi}$ of the cylinder (dashed curve) and the bush $\dot{\varphi}$ (solid curve) versus the dimensionless time τ for considered cases 4 and 5 is presented. In case 4, the system shows stick-slip oscillation ($T = 0.642$). In case 5 the oscillation exhibited by system is of the thermal stick-slip type ($T = 4.49$). Recall that the root of the characteristic equation responsible for instability yields the approximated period $T = 2\pi/\mathrm{Im}s_1 = 4.58$.

In Figures 6 and 7, time histories of both the contact pressure and the temperature for the considered cases are shown using solid curves 1–5. In cases 4 and 5, the contact characteristics undergo changes in time.

Analysis of the Braking Process ($m_0 = 0$)

It is assumed that at the initial state the shaft rotates with angular velocity $\dot{\phi}^\circ$ ($h_M(\tau) = 0$). The dimensionless temperature of the bush changes in agreement with the formula $h_T(\tau) = 1 - \exp(-\delta\tau^2)$. Owing to the heat transfer, the rotating cylinder expands and comes into contact with the bush; that is, braking occurs. The initial conditions are $\varphi^\circ = 0$, $\omega^\circ = 0$, $\phi^\circ = 0$, and $\dot{\phi}^\circ = 100$. The computational examples are shown in Figures 8–10 for some values of the parameter γ. Curve 1 corresponds to the case $Bi = 10$, $\tilde{\omega} = 0.1$, $\gamma = 1.87$, whereas curve 2 represents the case $Bi = 10$, $\tilde{\omega} = 0$, $\gamma = 1.87$ (the bush does not oscillate). In Figure 8, the dimensionless time histories of the dimensionless angular velocity of the shaft $\dot{\phi}$ (dashed curves) and the bush $\dot{\varphi}$ (solid curves) during the braking process are shown. It is seen (curve 1) that the shaft angular velocity decreases, and the bush undergoes oscillations until the two angular velocities reach the same value. Because there is not any moment applied and the damping has not been introduced, the bush and the shaft start to oscillate as one body with the period $T = 2\pi/\omega_0$. When the bush dynamics is not

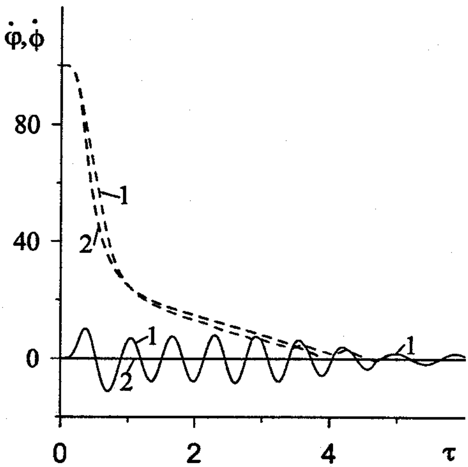

Figure 8. Time history of the braking pad angular speed $\dot{\varphi}$ (solid curves) and the shaft speed $\dot{\phi}$ (dashed curves) during braking ($m_0 = 0$) for various values of $\tilde{\omega}$. Curve 1, $\tilde{\omega} = 0.1$; curve 2, $\tilde{\omega} = 0$.

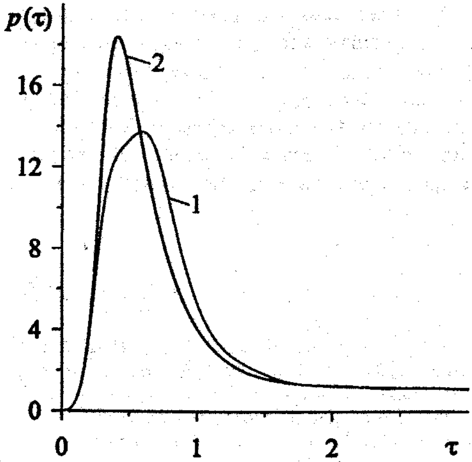

Figure 9. Time history of contact pressure during shaft braking ($m_0 = 0$) for various values of $\tilde{\omega}$. Curve 1, $\tilde{\omega} = 0.1$; curve 2, $\tilde{\omega} = 0$.

taken into account ($\tilde{\omega} = 0$, see curve 2), the shaft velocity also decreases and finally the shaft stops. The comparison of the results represented by curves 1 and 2 leads to the conclusion that the shaft braking time for $\tilde{\omega} = 0$ is smaller than the time interval needed for the shaft and bush to achieve a fixed contact (stick) with each other ($\tilde{\omega} = 0.1$). In Figures 9 and 10, time histories of the contact pressure and the

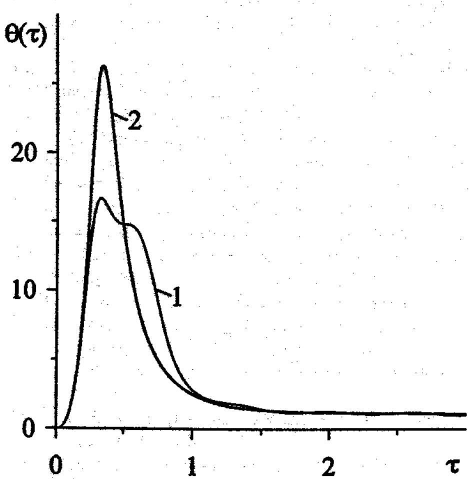

Figure 10. Time history of contact temperature during shaft braking ($m_0 = 0$) for various values of $\tilde{\omega}$. Curve 1, $\tilde{\omega} = 0.1$; curve 2, $\tilde{\omega} = 0$.

temperature are presented. Both characteristics increase in the beginning when $\gamma > 0$ (see curves 1 and 2). It can be concluded that during the braking process the maximum values of the pressure and the contact temperature become smaller when the dynamics of the bush is taken into account.

CONCLUSIONS

One of the classical models of an elastically supported braking pad being in frictional contact with a rotating shaft during frictional heat generation and heat expansion is analyzed with the use of the Stribeck friction model. The stability analysis of the stationary solutions is followed by the numerically verified analytical estimation of the periodic stick-slip occurrence. It is detected and illustrated that the stick-slip motion appears in the existence of the driving moment, heat transfer, and thermal expansion of the shaft materials. In addition, numerical calculations illustrating the influence of the parameters on the dynamics and on the contact characteristics of the investigated model in the acceleration and braking processes were performed.

It should be emphasized that, contrary to the results reported in the literature [17] where, already at a small wear, the frictional TEI occurs (contact parameters increase exponentially after the relative speed exceeds the critical value, which is found from the condition $v = 1$) and either an overheating [9,13,16] or a heating break [11,12] may appear, the considered system can never be overheated. An increase of the moment of friction force, frictional heat generation, and system heating is caused by an increase of the contact pressure while one of the contacting bodies moves with a constant speed and the heat expansion is bounded. To keep the motion speed constant, the moment of friction force increases and, consequently, energy is supplied to the system. Although the system heat expansion is bounded, the contact pressure may increase, which yields an increase of both the moment of friction force and the frictional heat generation. However, the system will not be overheated as the moving body starts to brake. The heat balance leads to a cooling process and, hence, the contact pressure and the moment of friction force start to decrease. This, however, again brings an increase in the relative speed and in the frictional heat generation. The described process will repeat again and again, which physically means that the system controls itself to avoid overheating. This type of control is called passive. In addition, it is suggested that the phenomena referred to as stick-slip in the classical terminology be called "thermal stick-slip" instead. This new terminology seems to be more adequate because a slip relates to a heating process caused by an independent movement of two bodies, whereas a stick corresponds to a process of cooling that takes place when the relative velocity of two contacting bodies equals zero. It is worth noticing that in the latter case, although the bush does not move, the shaft exhibits the thermal stick-slip dynamics.

When the frictional heat generation is not taken into account ($\gamma = 0$), the stick-slip oscillations cannot appear. In this case there are two stable stationary solutions, and one unstable, and, hence, any trajectory is always attracted by one of the stable critical points (equilibrium). For $\gamma > 0$, thermal stick-slip oscillation can appear, and then either a short bush oscillation period ($T = 0.642$ for case 4) or a long period, the one of shaft oscillations ($T = 4.49$ for case 5), is achieved. Owing to the dynamics of the considered system, the maximum pressure and the maximum temperature decrease during the braking process.

To conclude, in the system where the heat expansion of the contacting bodies is bounded, for the sake of stability it is better to apply the mechanical external excitation (considered here) than the kinematic excitation [17].

REFERENCES

1. J. R. Barber, Thermoelasticity and Contact, *J. Thermal Stresses*, vol. 22, pp. 513–525, 1999.
2. A. A. Andronov, A. A Vitt, and S. E. Khaikin, *Theory of Oscillations*, Pergamon Press, Oxford, 1966.
3. J. Awrejcewicz, I. V. Andrianov, and L. I. Manievich, *Asymptotic Approaches in Nonlinear Dynamics: New Trends and Applications*, Springer, Berlin, 1998.
4. I. Krahelskyy and N. Hittis, *Frictional Self-Oscillations*, Nauka, Moscow, 1987 (in Russian).
5. J. A. C. Martins, J. T. Oden, and F. M. F. Simões, A Study of Static and Kinetic Friction, *Int. J. Eng. Sci.*, vol. 28, pp. 29–92, 1990.
6. R. A. Ibrahim, Friction-Induced Vibration, Chatter, Squeal and Chaos Part 1-2: Mechanics of Contact and Friction, *Appl. Mech. Rev.*, vol. 47, pp. 209–227, 1994.
7. A. V. Chichinadze, E. D. Brown, A. H. Hinsburg, and Z. V. Ihnatyeva, *Calculation, Trial and Selection of Friction Couples*, Nauka, Moscow, 1979 (in Russian).
8. Yu. I. Neimark, *Maps Method in Theory of Nonlinear Oscillations*, p. 272, Nauka, Moscow, 1972 (in Russian).
9. Yu. Pyryev and D. Hrylitskyy, Transient Problem of Frictional Contact for the Cylinder with Heat Generation and Wear, *Appl. Mech. Tech. Phys.*, vol. 37, pp. 99–104, 1996 (in Russian).
10. Yu. Pyryev, Frictional Contact of the Cylinder and the Bush with Inertia, Heat Generation and Wear Taken into Account, *Physicochem. Mech. Mater.*, vol. 36, pp. 53–58, 2000 (in Russian).
11. D. V. Grylitskiy, Yu. Pyryev, and Yu. I. Mandzyk, Quasistatic Thermoelastic Contact Problem for Infinite Two-Layer Circular Cylinder under Friction Heating, *J. Thermal Stresses*, vol. 20, pp. 47–65, 1997.
12. Z. S. Olesiak and Yu. Pyryev, On Dynamical Thermoelastic Contact of Two Solids with Heat of Friction Generation and Wear, *Third International Congress on Thermal Stresses*, Krakow, Poland, pp. 599–602, June 130–17, 1999.
13. Z. S. Olesiak and Yu. A. Pyryev, On a Motion of Elastic Solids with Stick-Slip Effect and the Frictional Heat Generation, *Proceedings of the Fourth International Congress of Thermal Stresses*, pp. 589–592, Osaka, Japan, June 8–11, 2001.
14. Z. S. Olesiak and Yu. A. Pyryev, A Nonlinear, Nonstationary Problem of Frictional Contact with Inertia and Heat Generation Taken into Account, *Acta Mech.*, vol. 143, pp. 67–78, 2000.
15. Z. Olesiak, Yu. Pyryev, and A. Yevtushenko, Determination of Temperature and Wear During Braking, *Wear*, vol. 210, pp. 120–126, 1997.
16. J. R. Barber, T. W. Beamond, J. R. Waring, and C. Pritchard, Implications of Thermoelastic Instability for the Design of Brakes, *J. Tribology*, vol. 107, pp. 206–210, 1985.
17. J. Awrejcewicz and Yu. Pyryev, Thermoelastic Contact of a Rotating Shaft with a Rigid Bush in Conditions of Bush Wear and Stick-Slip Movements, *Int. J. Eng. Sci.*, vol. 40, pp. 1113–1130, 2002.
18. F. F. Ling, A Quasi-iterative Method for Computing Interface Temperature Distribution, *ZAMP*, vol. 10, pp. 461–474, 1959.
19. W. Nowacki, *Thermoelasticity*, 2nd ed., PWN—Pergamon Press, Warsaw, 1986.
20. H. S. Carslaw and J.C. Jaeger, *Conduction of Heat in Solids*, Clarendon Press, Oxford, 1959.